Eur. Phys. J. D **34**, 15–18 (2005)
DOI: 10.1140/epjd/e2005-00101-2

THE EUROPEAN PHYSICAL JOURNAL D

# Time-of-flight mass spectrometer coupled to a position sensitive detection

## Application to molecular beam deflection and photofragmentation experiments

M. Abd El Rahim, R. Antoine, L. Arnaud, M. Broyer, D. Rayane, A. Viard, and Ph. Dugourd[a]

Laboratoire de Spectrométrie Ionique et Moléculaire, UMR 5579 Université Lyon I et CNRS,
43 boulevard du 11 novembre 1918, 69622 Villeurbanne Cedex, France

Received 6 September 2004
Published online 13 July 2005 – 

**Abstract.** In this article we present the first results that we have obtained with a time-of-flight mass spectrometer coupled to a position sensitive detector. This new spectrometer provides a three-dimensional imaging ($X$ and $Y$ positions and time-of-flight) of the ion packet on the detector, with a high acquisition rate and a high resolution on both the mass and the position. This new apparatus is used to measure the electric deflection of PABA (p-amino benzoic acid) and PABA dimer beams and to study the kinetic energy release of the photofragmentation of the PABA dimer.

**PACS.** 39.10.+j Atomic and molecular beam sources and techniques – 33.15.Kr Electric and magnetic moments (and derivatives), polarizability, and magnetic susceptibility

## 1 Introduction

Different position sensitive detections (PSD) coupled to time-of-flight mass spectrometry have been developed for molecular beam experiments. The main application concerns collision experiments (ion–molecule reactions, coulomb explosion, cluster fragmentation...) [1]. Recently, the development of more complex data acquisition and storage schemes with multi-hit capability and of trigged CCD camera has given a new impulse to the field of atomic and molecular collisions and has opened new applications. A field, where position sensitive detection is needed, is molecular beam deflection experiments [2,3]. However, up to recently, it has never been developed for this field.

We have built a high resolution time-of flight mass spectrometer coupled to a position sensitive detection based on microchannel plates and delay lines [4]. This spectrometer allows one to read simultaneously and fast the 2D position and the arrival time of the ions which hit the detector and is applied to molecular beam electric deflection experiments. In this paper, we describe the first results obtained with this new apparatus. Two applications are discussed. First, the use of PSD for molecular beam deflection experiments with the deflection of p-amino benzoic acid (PABA) molecules and of PABA dimers. The second application is the observation of the kinetic energy release during the photofragmentation of a molecule or a complex.

[a] e-mail: dugourd@lasim.univ-lyon1.fr

## 2 Experiment

A schematic of the experimental apparatus is shown in Figure 1. It consists of a molecular beam source coupled to an electric deflector and time-of-flight mass spectrometer (TOFMS).

The molecular beam is produced by a laser vaporization source. The third harmonic of a $Nd^{3+}$:YAG laser is

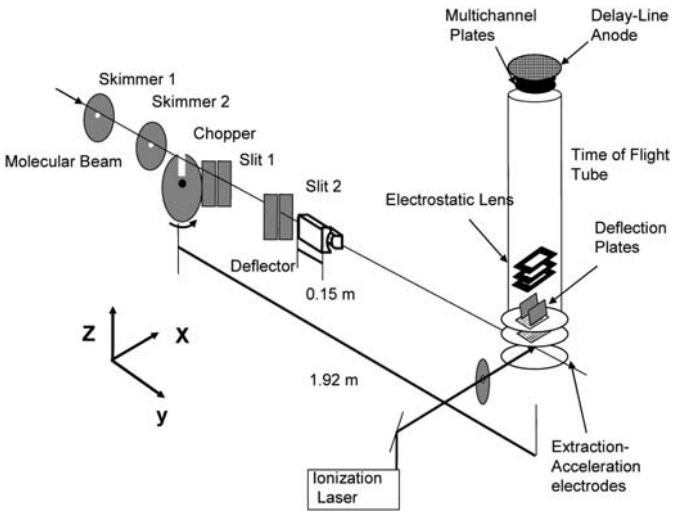


**Fig. 1.** Schematic overview of the molecular beam deflection/time-of-flight mass spectrometer/position sensitive detection experiment. In the deflector, $F$ and $\nabla F$ are along the $X$-axis.

used for the laser ablation of a cylindrical rod that is rotated and translated in a screw motion. A short pulse of helium or neon is synchronized with the ablation laser. The molecular beam leaves the source through a 5 cm long nozzle. After two skimmers (1.5 mm and 2 mm diameters), the beam is collimated by two rectangular slits (∼0.35 mm width and separated by 0.6 m) and travels through the two poles of the electric deflector. The poles of the deflector are two 15 cm long cylinders which are 1.7 mm apart. The geometry provides an inhomogeneous electric field which is equivalent to an "electrical two-wire field". The electric field and its gradient at the center of the deflector are $F = 1.63 \times 10^7$ Vm$^{-1}$ and $\nabla F = 2.82 \times 10^9$ Vm$^{-2}$, for a voltage of $U = 27$ kV across the two poles ($F$ and $\nabla F$ are along the $X$-axis). The beam undergoes a deflection on the $X$-axis which is measured 1.025 m after the deflector. The deflection $d$ of a particle is:

$$d = K \frac{\langle \mu_x \rangle_{F,T} \nabla F}{mv^2} \quad (1)$$

where $\langle \mu_x \rangle_{F,T}$ is the average value of the $X$-component of the dipole of the particle in the electric field and at temperature $T$. $K$ is a constant depending on the geometry of the apparatus, m the mass, and $v$ the velocity of the molecule. The beam velocity $v$ is selected and measured with a mechanical chopper located in front of the first slit.

1.025 m after the deflector, the neutral particles enter the extraction region of linear time-of-flight mass spectrometer and are ionized by a pulsed nanosecond laser beam. The MS is perpendicular to the axis of the neutral molecular beam ($Y$-axis) and to the pulsed ionization laser ($X$-axis). It consists of an extraction region, an acceleration region, two deflection electrodes, an electrostatic lens and a free flight region. Wires parallel to the $X$-axis are used to define the boundaries of the extraction and acceleration regions. Standard Wiley-MacLaren conditions of focalization are used during these experiments [5]. The electrostatic lens is located ∼30 cm after the extraction region. It has been specially designed to magnify the ion image on the $X$-axis without modification on the $Y$-axis. The magnification factor is $G$ and the deflection $D$ of a molecule observed on the detector is equal to:

$$D = Gd = GK \frac{\langle \mu_x \rangle_{F,T} \nabla F}{mv^2}. \quad (2)$$

The value of GK was calibrated with a lithium atomic beam [6].

The detector is located 1 meter after the acceleration plate. It is a pair of microchannel plates coupled to two orthogonal delay lines. The arrival time at the detector and the position on the detector are recorded for each ion. The detector, its electronic and the data processing are discussed in [6].

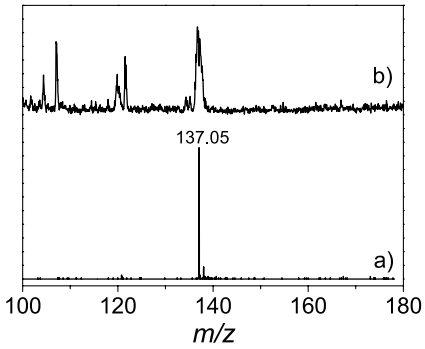


**Fig. 2.** TOF mass spectra recorded for PABA ($M = 137$). (a) Present work $U_{Ext} = 370$ V, $U_{Acc} = 3500$ V (the resolving power $M/\Delta M$ is ∼3000). (b) Mass spectrum recorded with a position sensitive time of flight used previously for electric deflection experiments $U_{Ext} = 1000$ V, $U_{Acc} = 3500$ V (the resolving power $M/\Delta M$ is ∼100).

## 3 Application to molecular beam deflection experiments

### 3.1 The p-amino benzoic acid

We first discuss the electric deflection of the isolated PABA molecule in its ground state. Due to an electron transfer from the animo group to the acid group, this molecule has a strong permanent dipole. The value of the dipole moment along the principal axis of the molecule was measured by Compagnon et al. ($\mu_A = 2.8 \pm 0.2$ D) [7]. Figure 2a shows a mass spectrum obtained by vaporizing a rod made of PABA (30% of mass ratio) and cellulose. The source conditions (delays, pressure and laser power) were adjusted in order to produce a beam of PABA molecules without any clusters. The peaks at $M = 137$ and $M = 138$ correspond to the two main isotopes of the PABA molecule. These two peaks are well resolved. As a comparison, Figure 2b shows the mass resolution obtained with our previous apparatus. For this spectrum, the extraction and acceleration voltages were adjusted in order to measure the deflection from the arrival time at the detector [8]. The increase in resolving power is significant and opens new possibilities, in particular deflection experiments on clusters or molecules which are observed in congested mass spectra.

Figure 3a shows the image of the PABA ions ($M = 137$) on the detector. The ion packet is spread on the $Y$-axis. This is due to the wires used on the extraction and acceleration electrodes. Indeed, when different electric fields are placed on each side of a wire layer or a grid, a small electrostatic lens is produced at each opening which modifies the ion trajectories [9,10]. The image is well resolved on the $X$-axis. The width of the image on this axis corresponds to the width of the molecular beam multiplied by the magnification factor provides by the electrostatic lens ($G$).

Figure 3b shows the image of the ion packet recorded for the PABA molecule with $F = 1.51 \times 10^7$ V/m in the deflector. The profile of the beam on the $X$-axis measured

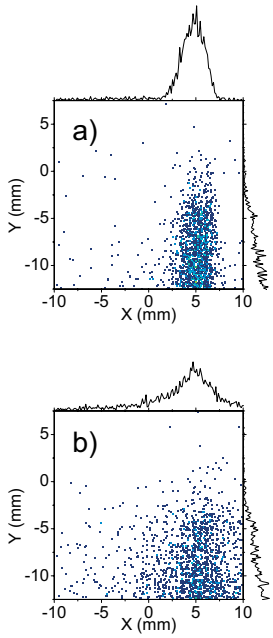


**Fig. 3.** Experimental 2D $X-Y$ image of PABA ions on the PSD system. The projections on the $X$-axis and $Y$-axis are also plotted. (a) $F = 0$ in the deflector. (b) $F = 2.4 \times 10^6$ V/m. The velocity of the beam was 753 ms$^{-1}$ (neon was used as carrier gas, $T = 300$ K). The shift in the initial position of the beam in $X$-direction is due to the alignment of the experiment and the shift of the beam in the $Y$-direction to the velocity of the molecular beam.

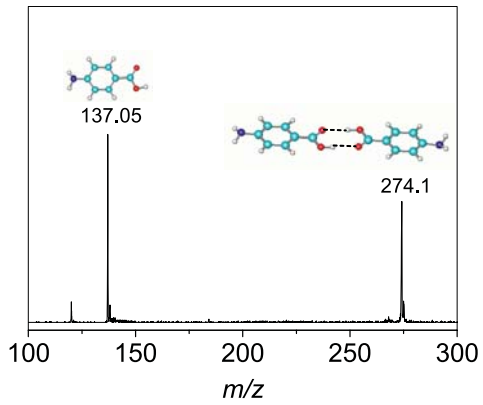


**Fig. 4.** TOF mass spectra of PABA monomers ($M = 137$) and PABA dimers ($M = 274$). The structures of the molecule and of the complex are shown.

with the electric field is symmetrically broadened. For a rigid rotor, the average value $\langle \mu_x \rangle_{F,T}$ and then the deflection $D$ depends on the rotational level of the molecule. The simulation of the rotational motion of the molecule in the electric field and of the broadening of the beam is discussed in details in references [7,11]. The present measurements are in agreement with previous results [7]. The major improvement of the new apparatus is the high mass resolution obtained simultaneously with a direct measurement of the beam profile for each mass value.

### 3.2 PABA dimer

The dimer of PABA is made of two para-aminobenzoic acid molecules which are weakly bound by two hydrogen bonds. Figure 4 shows a mass spectrum recorded with the source conditions adjusted to produce dimers in the beam. The most intense peak ($M = 274$) corresponds to

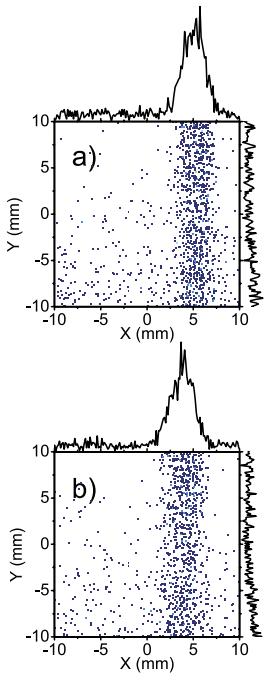


**Fig. 5.** Experimental 2D $X-Y$ image of PABA dimer ions on the PSD system. The projections on the $X$-axis and $Y$-axis are also plotted. (a) $F = 0$ in the deflector. (b) $F = 1.51 \times 10^7$ V/m. The velocity of the beam was 716 ms$^{-1}$ (neon was used as carrier gas, $T = 300$ K).

the dimer. Images of the ion packets ($M = 274$) recorded with and without electric field in the deflector are displayed in Figure 5. In this case, the electric field does not induce a broadening of the beam but a global deflection of the beam ($D = 1.3$ mm). At equilibrium the geometric structure of the dimer is symmetrical (see insert in Fig. 4) and the permanent dipole is zero. When the temperature increases, the molecule vibrates. In an altered conformation, the dipole may be non null. In the deflector, the average value of the dipole of the molecule on the axis of the electric field is given by the Langevin-Debye formula [12,13]:

$$\langle \mu_x \rangle = \left[ \alpha_{e-} + \frac{\langle \mu^2 \rangle_{T,F=0}}{3kT} \right] F_x = \chi F_x. \qquad (3)$$

The susceptibility deduced from the deflection measured in Figure 5 is 82 Å$^3$ which is in perfect agreement with previous results [14].

## 4 Photofragmentation and kinetic energy release measurement of the PABA dimer

By increasing the power of the ionization laser it is possible to fragment efficiently the complex. The ratio of monomers over dimers increases linearly with the laser power in agreement with a three photons process: two for ionization and one for fragmentation. The fragmentation leads to a neutral and a charged PABA molecules. This second fragment is detected on the monomer mass channel. Figure 6 compares the profile of the beam measured for $M = 274$ (dimer mass channel) and for $M = 137$ (monomer mass channel) obtained using a high ionization laser power. In Figure 6b, the contribution coming

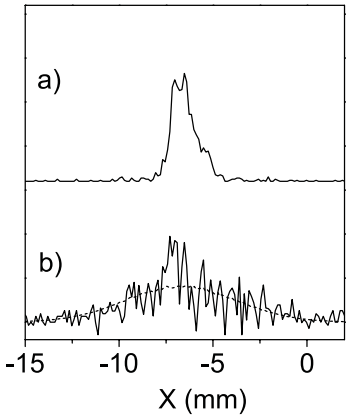


**Fig. 6.** (a) Projection on the $X$-axis of the ion image measured on the dimer mass channel. (b) Projection on the $X$-axis of the ion image measured on the monomer mass channel. This image results from the fragmentation of the dimer (the contribution of initial monomers has been substracted). The dashed line shows the result of a simulation using a Maxwell Boltzmann distribution for the kinetic energy release with $T = 700$ K.

from the monomers present in the molecular beam has been substracted. This peak is much broader than the one displayed in Figure 6a. The kinetic energy release occurring during the dissociation broadens the initial well collimated beam. The kinetic energy release can be calculated with the Langevin collision model. For a polarization potential between the two fragments, the kinetic energy release follows a Maxwell Boltzmann distribution [15,16]. The adjustment of the temperature of this distribution on the experimental curve displays in Figure 6b leads to $T = 700 \pm 200$ K. If one considers than the dissociation is due to the absorption of a third photon (the first two photons are needed for ionization), and if one assumes an initial temperature of 300 K and a statistical distribution of the excess energy, the expected temperature is $\sim$800 K. This is in agreement with the experimental kinetic energy release, which is in favor of a thermalization of the complex before fragmentation.

In conclusion, we have demonstrated that the deflection of a molecular beam by an inhomogeneous electric field can be measured with a TOF-MS coupled to a PSD. The same apparatus can be used for magnetic deflection experiments. By this technique the deflection is measured without decreasing the resolving power of the mass spectrometer. This detection also allows the measure of kinetic energy release and opens new perspectives for the study of electric and magnetic properties of complex molecules.

## References

1. J. Ullrich, R. Moshammer, R. Doerner, O. Jagutzki, V. Merge, H. Schmidt-Boecking, L. Spielberger, J. Phys. B **30**, 2917 (1997)
2. K.D. Bonin, V.V. Kresin, *Electric-Dipole Polarizabilities of Atoms, Molecules and Clusters* (World Scientific, Singapore, 1997)
3. M. Broyer, R. Antoine, E. Benichou, I. Compagnon, P. Dugourd, D. Rayane, C.R. Phys. **3**, 301 (2002)
4. O. Jagutzki, V. Mergel, K. Ullmann-Pfleger, L. Spielberger, U. Meyer, R. Dörner, H. Schmidt-Böcking, Proc. SPIE **3438**, 322 (1998)
5. W.C. Wiley, I.H. McLaren, Rev. Sci. Instrum. **26**, 1150 (1955)
6. M. Abd El Rahim, R. Antoine, L. Arnaud, M. Barbaire, M. Broyer, C. Clavier, I. Compagnon, P. Dugourd, J. Maurelli, D. Rayane, Rev. Sci. Instrum. **75**, 5221 (2004)
7. I. Compagnon, R. Antoine, D. Rayane, M. Broyer, P. Dugourd, J. Phys. Chem. A **107**, 3036 (2003)
8. W.A. deHeer, P. Milani, Rev. Sci. Instrum. **62**, 670 (1991)
9. S.M. Colby, C.W. Baker, J.J. Manura, *Proceedings of the 41st ASMS Conference on Mass Spectrometry and Allied Topics*, San Francisco, CA., 1996
10. T. Bergmann, T.P. Martin, H. Schaber, Rev. Sci. Instrum. **60**, 347 (1989)
11. P. Dugourd, I. Compagnon, F. Lepine, R. Antoine, D. Rayane, M. Broyer, Chem. Phys. Lett. **336**, 511 (2001)
12. P. Debye, *Polar molecules* (Dover Publications, New York, 1929)
13. J.H.V. Vleck, Phys. Rev. **30**, 31 (1927)
14. I. Compagnon, R. Antoine, D. Rayane, M. Broyer, P. Dugourd, Phys. Rev. Lett. **89**, 253001 (2002)
15. H.J. Hwang, D.K. Sensharma, M.A. El-Sayed, Chem. Phys. Lett. **160**, 243 (1989)
16. C.E. Klots, J. Chem. Phys. **64**, 4269 (1976)